A comparison of oxide decay heat simulations and nuclear data libraries with fusion irradiation experiments

L W Packer[1], M Angelone[2], M R Gilbert[1], S Loreti[2], C R Nobs[1] M Pillon[2], J-C Sublet[3] and O Vilkhivskaya[1]

[1]UK Atomic Energy Authority
Culham Science Centre, Abingdon, Oxon, OX14 3DB, UK

[2]ENEA - Department of Fusion and for Nuclear Safety and Security
via E. Fermi 45, 00044 Frascati (Rome), Italy

[3]International Atomic Energy Agency
PO Box 100, 1400 Vienna, Austria

lee.packer@ukaea.uk, maurizio.angelone@enea.it, mark.gilbert@ukaea.uk, stefano.loreti@enea.it, chantal.nobs@ukaea.uk, mario.pillon@enea.it, j.c.sublet@iaea.org, olga.vilkhivskaya@ukaea.uk

ABSTRACT

We compare existing experimental decay heat data sets measured at the JAEA fusion neutron source (FNS), which employed a fast extraction rabbit system that in certain cases allowed the measurements to capture, at short cooling times, the decay profile of ^{16}N in a range of oxides. Focussing on those data points and timescales that can be attributed to ^{16}N, we compare measurements to simulations performed using the FISPACT-II inventory code together with evaluated nuclear data libraries. Making small corrections for other contributions at these short times, we derive integral cross section data estimates for ^{16}O(n,p)^{16}N from 12 oxide sample measurements and compare with previously obtained measurements in the IAEA EXFOR database and evaluations in the nuclear data libraries themselves.

KEYWORDS: decay heat, oxide activation, cross section

1. INTRODUCTION

Cooling water in the primary circuit in both fission and fusion nuclear reactors is unavoidably exposed to neutrons leading to the generation of problematic short-lived isotopes, most importantly, ^{16}N ($T_{1/2}$=7.3s) via the ^{16}O(n,p)^{16}N reaction. This presents a significant itinerant radiation source to consider for operational dose and impact on radiation sensitive equipment, such as electronics and cryogenic components such as superconducting magnets, particularly due to the intense 6.13 MeV gamma ray that is emitted during ^{16}N decay. This issue is well-known from water-cooled fission reactors [1], though in fusion devices such as ITER, where water coolant will be used extensively in first wall and other components throughout the device, the intensity of the phenomena

is expected to be more severe. The reasons for this is partly because the neutron energy threshold of the ^{16}O(n,p)^{16}N reaction (the primary pathway to the production of ^{16}N) is above 10 MeV, and D–T fusion neutrons are born around 14 MeV energy. ITER is designed to operate at 500 MW fusion power, where the 14 MeV neutron emission rates from the deuterium-tritium plasma will be 1.77×10^{20} n s^{-1} and the neutron fluence experienced by some first wall water-cooled components will exceed 10^{14} n cm^{-2} s^{-1}. Presently due to uncertainties in modelling and nuclear cross section data large safety factors, between 8.2 and 4.7, are applied within the ITER project. Activities are ongoing to seek experimental justification to reduce these factors via coolant loop experiments at the Frascati Neutron Generator [2–4], which has incorporated an ITER first wall mock up component incorporating water coolant channels, irradiated with 14 MeV neutrons and the ^{16}N emissions measured via a high efficiency CsI detector at different water flow rates.

To complement to the body of work on this important phenomena, in this paper we provide new insight from experimental decay heat data sets measured at the JAEA 14 MeV fusion neutron source (FNS) [5–7] with irradiated samples where the ^{16}O(n,p)^{16}N reaction contributes to decay heat. The FNS experimental campaigns employed a fast extraction rabbit system that in certain cases allowed the measurements to capture, at short cooling times, the decay profile of ^{16}N in a range of oxides: As_2O_3, Cs_2O_3, CaO, Er_2O_3, Eu_2O_3, Gd_2O_3, GeO_2, La_2O_3, Lu_2O_3, Tb_4O_7, Tm_2O_3, Yb_2O_3. Focussing on those data points and timescales that can be attributed to ^{16}N, we have compared measurements to simulations performed using the FISPACT-II [8,9] inventory code together with the TENDL-2017 nuclear data library [10]. Extensive decay heat analysis and comparison with the FISPACT-II inventory code using various nuclear data libraries has been performed in [11]. However, here we provide analyses to derive integral cross section data estimates for ^{16}O(n,p)^{16}N from 12 oxide sample measurements and compare with previously obtained measurements in the IAEA EXFOR database and evaluations in the nuclear data libraries themselves.

Figure 1 shows a comparison of cross section libraries for the ^{16}O(n,p)^{16}N reaction using EAF-2010, JENDL-4.0 and ENDF/B-VIII/JEFF-3.3/TENDL-2017 libraries. Data points are experimental data with uncertainties from EXFOR. The cross section shows the energy threshold, above 10 MeV. The evaulations are fairly consistent around 14 MeV, though larger differences between JENDL-4.0 and the other libraries can be seen in the energy region between 11 and 12 MeV.

2. Description of FNS experiments

14 MeV neutrons were generated at the JAEA FNS facility via a 2 mA deuteron beam incident on tritium loaded titanium target. A series of experiments took place between 1996–2000 where thin samples, nominally 25×25 mm^2 in area, and approximately 10 μm thick were irradiated for 5 minutes in a neutron flux typically in range 10^9– 10^{10} n cm^{-2} s^{-1}. Figure 1 (right-hand y-scale) shows a calculated neutron spectrum at the FNS at the irradiation position. Full details of the earlier of these experimental campaigns are provided in [5–7] with details from the 2000 experiments analysed in [11]. A sample irradiation 'stack' comprising the irradiation sample together with an Al monitor foil were placed into a plastic 'rabbit' capsule for each irradiation. The decay heat from the irradiated sample post-irradiation was measured using a Whole Energy Absorption Spectrometer (WEAS)—a system based on two large bismuth-germanate BGO ($Bi_4Ge_3O_{12}$) scintillators, associated photo-multiplier tubes, high voltage and pulse counting electronics, and a multi-channel analyser. Decay heat from both β^- and γ emissions were measured from the irradiated samples,

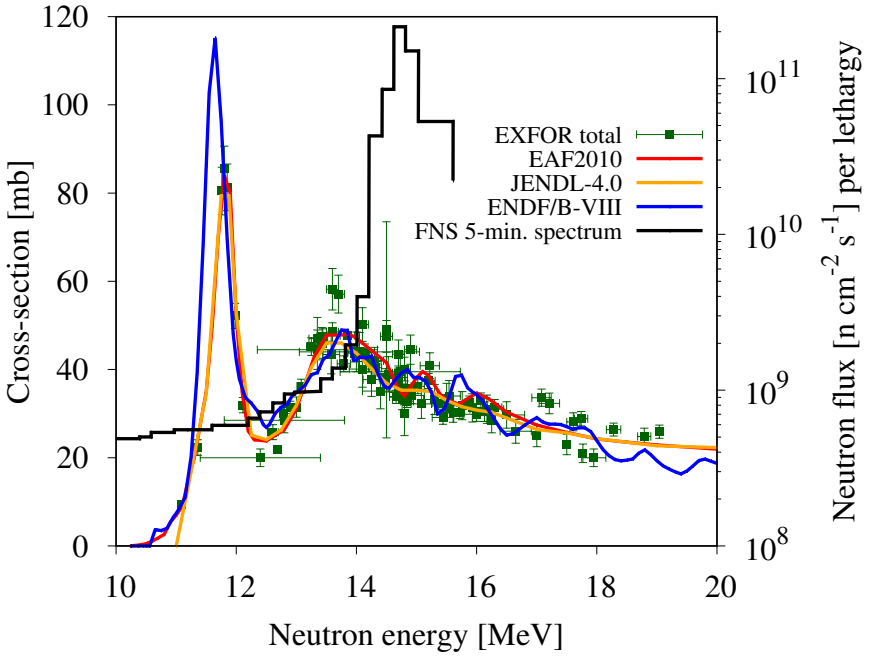

Figure 1: Comparison of cross section libraries for the ^{16}O(n,p)^{16}N reaction using EAF-2010, JENDL-4.0 and ENDF/B-VIII libraries (ENDF-B/VIII is adopted for JEFF-3.3 and TENDL-2017, since the libraries are identical). Data points are experimental data with uncertainties from EXFOR. The FNS 5 minute neutron flux spectrum is also shown for comparison with flux per lethargy on the right-hand y-scale.

typically 30-50 s following the end of the irradiation. Important to the design, the BGO scintillator does not suffer with hygroscopic degradation (as is the case with NaI scintillators) and hence encapsulation or 'window' materials are not needed. The lack of 'window' materials means that energy loss, particularly from β^- emissions, are minimal. Thin samples were centrally located between the detectors in a tight 'sandwich' arrangement (gap width was approximately 1 mm), with close to 4π sr counting geometry, giving almost 100 % efficiency. The samples were measured for several minutes, dumping data into periodic time bins (typically 16 seconds) which allowed the decay heat response to be monitored. Some samples were in powder form (CaO, for example) and in these cases the powder was spread uniformly and encapsulated in plastic adhesive tape. Blank tape samples were irradiated to subtract background decay heat. The irradiated Al monitor foil ^{24}Na activity was separately measured following each irradiation using a high-purity germanium detector; the ^{27}Al(n,α)^{24}Na reaction was used to determine the total D–T neutron fluence.

3. Analyses methodology

We have focussed on a subset of the data obtained in the year 2000 experimental campaign—a set of 12 oxide materials; As_2O_3, Cs_2O_3, CaO, Er_2O_3, Eu_2O_3, Gd_2O_3, GeO_2, La_2O_3, Lu_2O_3, Tb_4O_7, Tm_2O_3 and Yb_2O_3. Figure 2 (see the bottom plot) shows an example of decay heat measurements taken over the first three minutes of cooling for the Tm_2O_3 sample measurement. We have com-

pared the data with a calculation of the equivalent experimental scenario using the FISPACT-II code and the TENDL-2017 nuclear data library. In general we have concentrated on using experimental data points and timescales that can largely be attributed to ^{16}N. In this case for Tm_2O_3, and similarly in other cases analysed in this paper, the first data point that is highlighted at 0.6 minutes cooling (the shortest measurement time following irradiation). Since there are other contributions to decay heat from other nuclides (usually small in the cases studied here), other than the contribution from ^{16}N emissions, we have estimated these contributions at the relevant cooling time using the FISPACT-II code together with the TENDL-2017 nuclear data library so that corrections can be made in our later analyses to estimate ^{16}O(n,p)^{16}N cross sections. In the example case for Tm_2O_3 the contribution to decay heat from ^{16}N at 0.6 minutes is predicted to be 99.4 $\%$, with the remaining, rather small contribution, mostly coming from ^{168}Tm. The various contributions at different cooling times post-irradiation are illustrated in this case by the top plot shown in figure 2, which indicates that at longer cooling times, $>$1.5 minutes, ^{168}Tm dominates, with minor contributions from ^{166}Ho and ^{170}Tm. In another example, at the other end of the scale in these studied cases, for Eu_2O_3 (see figure 3), the contribution to decay heat from ^{16}N at 0.85 minutes cooling is much larger, 51.2 $\%$ with the remainder from ^{152n}Eu, ^{152m}Eu and ^{150m}Eu contributions. These other contributions can be partly explained by the later first measurement point at 0.85 minutes, compared to 0.6 minutes in all other cases studies in this paper. The time difference is about 15 seconds, which exceeds two half lives decay of ^{16}N. In general, throughout our analyses we have accounted for these corrections in an expanded uncertainty estimate, which accounts for both the measurement uncertainty and the decay heat correction from other isotopic contributions—here added in quadrature. The uncertainty estimate is likely to be an overestimate, since it implies no knowledge of cross sections from other reactions; we have effectively treated these correction with a 100 $\%$ uncertainty estimate.

To enable the measured (and corrected) decay heat to be converted into activity we have used the Q value for ^{16}N decay, which is 10438.869 $\pm$58.844 per disintegration [12], with 7263.658 $\pm$52.302 of this attributed to the absorbed quantity (the total calculated energy minus the neutrino energy). The absorbed value has been used to convert the measured total decay heat, corrected for ^{16}N contribution, to activity in Bq. A further correction factor of 0.9588 [7] has been applied to correct for the BGO decay heat measurement efficiency for ^{16}N emissions. Activity estimates for ^{16}N have then been decay corrected to the end of the irradiation period so that cross section estimates can be made via the following

$$\sigma = \frac{A_\infty}{\phi N_{^{16}O}} \tag{1}$$

where A_∞ is the saturated activity of ^{16}N, ϕ is the neutron flux and $N_{^{16}O}$ is the number of ^{16}N atoms cm^{-3} within the sample. The irradiation time, 5 minutes, is sufficiently long compared to the half-life of ^{16}N (7.13 s) that the saturated activity assumption can be made.

4. Results

Figure 4 shows the derived cross sections for As_2O_3, Cs_2O_3, CaO, Er_2O_3, Eu_2O_3, Gd_2O_3, GeO_2, La_2O_3, Lu_2O_3, Tb_4O_7, Tm_2O_3 and Yb_2O_3. The weighted average for these 12 results is 33.1 $\pm$16.6 mb. This compares with a spectrum averaged value of 33.6 mb using the TENDL-2017 library.

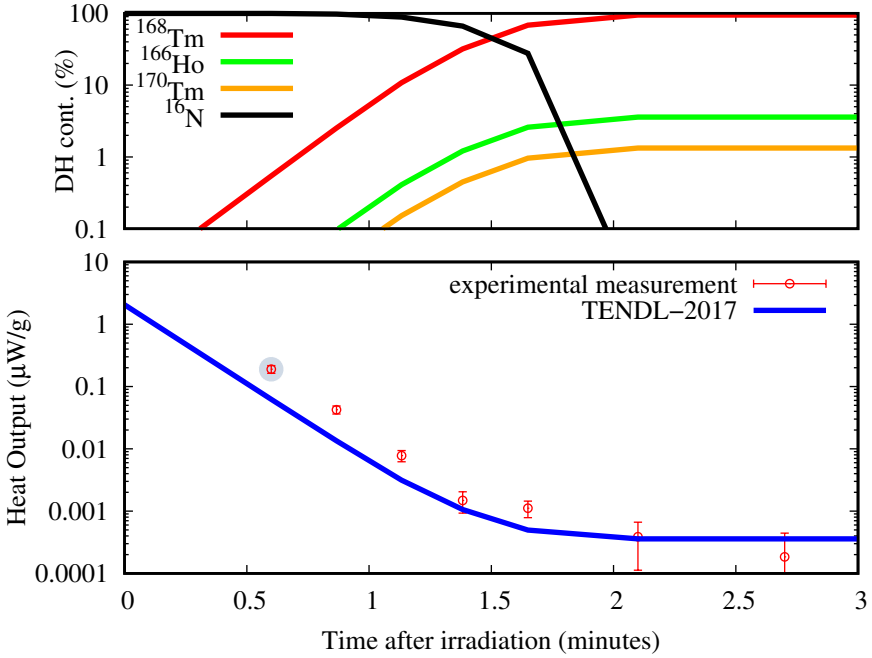

Figure 2: First 3 minutes cooling following the 5 minute irradiation for Tm_2O_3. The bottom plot shows measured decay heat values and uncertainties compared to FISPACT-II calculations using TENDL-2017. The circled experimental data point (the first measured point at 0.6 minutes) has been used to extract cross section in the analysis. The top plot shows the contribution to total decay heat by nuclide. At 0.6 minutes after irradiation ^{16}N contributes 99.67% of the total decay heat

5. Discussion and Conclusions

In this paper we have used experimental decay heat data sets measured at the JAEA fusion neutron source (FNS) to derive ^{16}O(n,p)^{16}N cross section estimates from the decay profile of ^{16}N in a range of oxides. Focussing on those data points and timescales that can largely be attributed to ^{16}N, we have compared measurements to simulations performed using the FISPACT-II inventory code together with evaluated nuclear data libraries. We have made small corrections for contributions to decay heat arising from contributions other than ^{16}N.

The spread in cross section results can be seen in Figure 4. In particular the estimates from the Cs_2O_3, Lu_2O_3, Tb_4O_7, and Yb_2O_3 measurements are higher than the other results presented. However, the measurement uncertainty associated with these samples were comparatively high, between 15 and 24 %. The overall weighted average integral cross section data estimate across the full 12 sample set was 33.1 $\pm$17.2 mb. This compares with a spectrum averaged value of 33.6 mb using the TENDL-2017 library and our result is therefore in good agreement. Given the narrow peak neutron energy of the FNS irradiation around 14.7 MeV one may also compare the weighted average result with differential experimental data shown in Figure 1 at 14.7 MeV. The EXFOR entries at 14.7 MeV are shown in Table 1. The weighted average of these four measurements is 36.8 $\pm$3.1 mb and also compares within uncertainties with the value determined through this work.

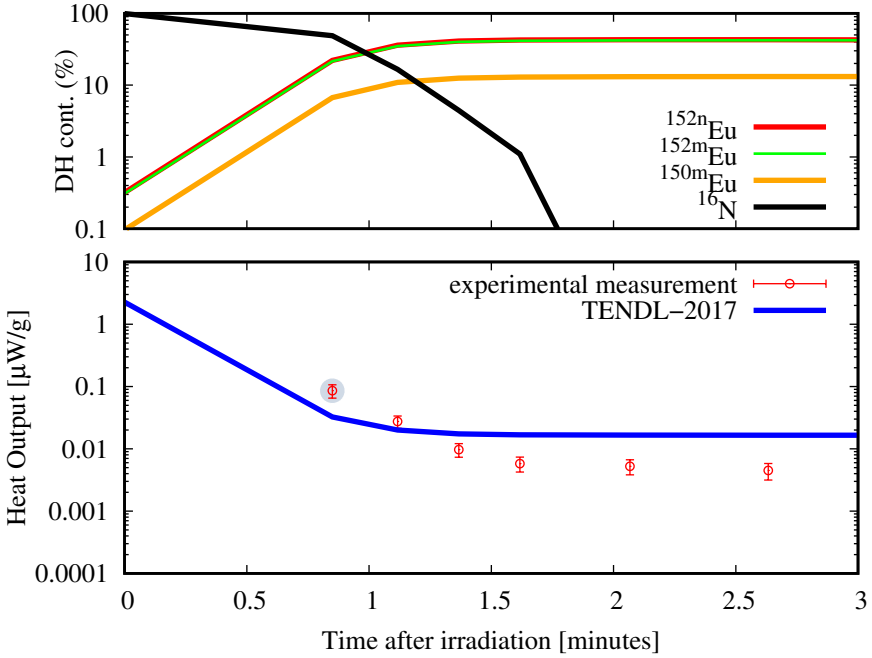

Figure 3: First 3 minutes cooling following the 5 minute irradiation for Eu_2O_3. The bottom plot shows measured decay heat values and uncertainties compared to FISPACT-II calculations using TENDL-2017. The circled experimental data point (the first measured point at 0.85 minutes) is used to extract cross section in the analysis. The top plot shows the contribution to total decay heat by nuclide. At 0.85 minutes after irradiation ^{16}N contributes 51.2% of the total decay heat

Table 1: EXFOR cross section measurements at 14.7 MeV.

EXFOR entry	Cross section [mb]	Δxs [mb]	ΔE [MeV]
DeJuren, 1960 (ID: 11411002)	39.2	1.6	0.1
Kantele, 1962 (ID: 11196004)	38.2	5.0	0.15
Schantl, 1970 (ID: 21846006)	34.8	1.1	0.15
Subashi, 2000 (ID: 22494002)	43.5	3.2	0.1
Weighted average	36.8	3.1	0.125

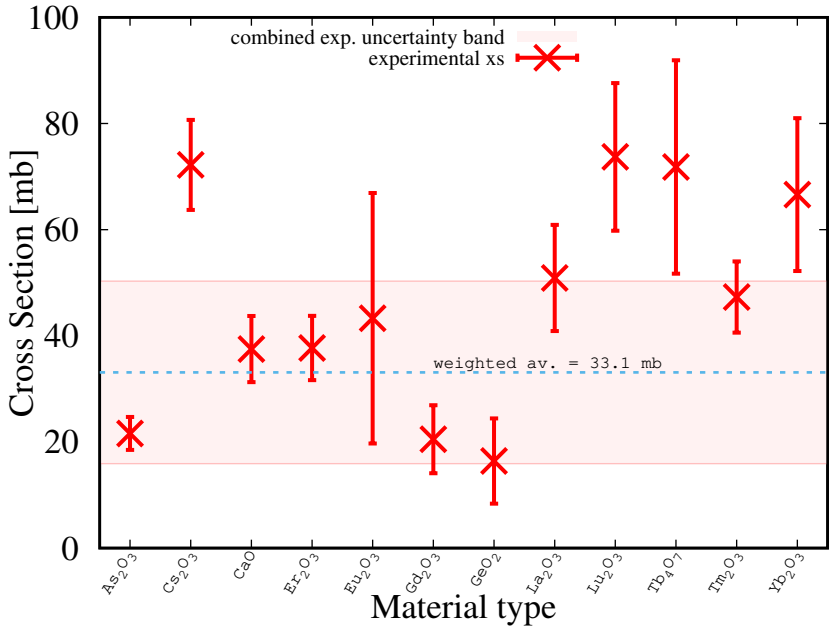

Figure 4: Experimental $^{16}O(n,p)^{16}N$ cross section from a range of oxides derived from decay heat experiments. The weighted average for all results is shown.

ACKNOWLEDGEMENTS

This work was funded by the RCUK Energy Programme [grant number EP/T012250/1]. To obtain further information on the data and models underlying this paper please contact publicationsmanager@ukaea.uk.

REFERENCES

[1] A. Žohar and L. Snoj. "On the dose fields due to activated cooling water in nuclear facilities." *Progress in Nuclear Energy*, **volume 117**, p. 103042 (2019).

[2] M. Pillon et al. "Comparison between measurement and calculations for a 14 MeV neutron water activation experiment. ND2019 conf. proc. Article in press." (2019).

[3] M. Angelone et al. "Measurement of Delayed Neutron Emission from Water Activated by 14 MeV Neutrons in a FW Mock-up of ITER. ISFNT-14 conf. proc. Article in press." (2019).

[4] C. R. Nobs et al. "Computational evaluation of N-16 measurements for a 14 MeV neutron irradiation of an ITER first wall component with water circuit. ISFNT-14 conf. proc. Article in press." (2019).

[5] F. Maekawa et al. "Compilation of benchmark results for fusion related nuclear data, Tech. Rep. JAERI-Data/Code 98-024, JAEA, 1998." URL http://www.jaea.go.jp/jaeri/.

[6] F. Maekawa et al. "Data collection of fusion neutronics benchmarking experiment conducted at FNS/ JAERI,Tech. Rep. JAERI-Data/Code 98-021, JAEA, 1998." URL http://www.jaea.go.jp/jaeri/.

[7] F. Maekawa, M. Wada, and Y. Ikeda. "Decay Heat Experiment and Validation of calculation code systems for fusion reactor, Tech. Rep. JAERI 99-055, JAEA, 1999." URL http://www.jaea.go.jp/jaeri/.

[8] J.-Ch. Sublet, J. W. Eastwood, and J. G. Morgan. "The FISPACT-II User Manual." Technical Report http://www.ccfe.ac.uk/assets/Documents/easy/CCFE-R(11)11.pdfCCFE-R(11) 11 Issue 6, CCFE (2014).

[9] J.-C. Sublet, J. Eastwood, J. Morgan, M. Gilbert, M. Fleming, and W. Arter. "FISPACT-II: An Advanced Simulation System for Activation, Transmutation and Material Modelling." *Nuclear Data Sheets*, **volume 139** (Supplement C), pp. 77 – 137 (2017). Special Issue on Nuclear Reaction Data.

[10] A. J. Koning and D. Rochman. " TENDL-2017. Release Date: April 25, 2018. Available from https://tendl.web. psi.ch/tendl 2017/tendl2017.html."

[11] M. R. Gilbert and J-C Sublet. "Experimental decay-heat simulation-benchmark for 14 MeV neutrons complex inventory analysis with FISPACT-II." *Nuclear Fusion*, **volume 69** (2019).

[12] J.H. Kelley et al. "Nuclear Physics A." **volume 564** (1993).